Biochimica et Biophysica Acta 1833 (2013) 3046–3053

Contents lists available at ScienceDirect

Biochimica et Biophysica Acta

journal homepage: www.elsevier.com/locate/bbamcr

Flow-induced activation of TRPV5 and TRPV6 channels stimulates Ca^{2+}-activated K^+ channel causing membrane hyperpolarization

Seung-Kuy Cha [a,b,*], Ji-Hee Kim [a], Chou-Long Huang [b,**]

[a] Department of Physiology, Institute of Lifestyle Medicine and Nuclear Receptor Research Consortium, Yonsei University Wonju College of Medicine, Wonju, Republic of Korea
[b] Department of Internal Medicine, UT Southwestern Medical Center, Dallas, TX 75390, USA

ARTICLE INFO

Article history:
Received 20 May 2013
Received in revised form 9 August 2013
Accepted 26 August 2013
Available online 31 August 2013

Keywords:
TRPV5
TRPV6
Flow-mediated Ca^{2+} entry
Ca^{2+}-activated K^+ channel
Flow-mediated K^+ secretion
ROMK

ABSTRACT

TRPV5 and TRPV6 channels are expressed in distal renal tubules and play important roles in the transcellular Ca^{2+} reabsorption in kidney. They are regulated by multiple intracellular factors including protein kinases A and C, membrane phospholipid PIP_2, protons, and divalent ions Ca^{2+} and Mg^{2+}. Here, we report that fluid flow that generates shear force within the physiological range of distal tubular fluid flow activated TRPV5 and TRPV6 channels expressed in HEK cells. Flow-induced activation of channel activity was reversible and did not desensitize over 2 min. Fluid flow stimulated TRPV5 and 6-mediated Ca^{2+} entry and increased intracellular Ca^{2+} concentration. N-glycosylation-deficient TRPV5 channel was relatively insensitive to fluid flow. In cells coexpressing TRPV5 (or TRPV6) and *Slo1*-encoded maxi-K channels, fluid flow induced membrane hyperpolarization, which could be prevented by the maxi-K blocker iberiotoxin or TRPV5 and 6 blocker La^{3+}. In contrast, fluid flow did not cause membrane hyperpolarization in cells coexpressing ROMK1 and TRPV5 or 6 channel. These results reveal a new mechanism for the regulation of TRPV5 and TRPV6 channels. Activation of TRPV5 and TRPV6 by fluid flow may play a role in the regulation of flow-stimulated K^+ secretion via maxi-K channels in distal renal tubules and in the mechanism of pathogenesis of thiazide-induced hypocalciuria.

1. Introduction

Mechanosensation is an important mechanism for cell communication with the external environment. Mechanosensitive ion channels play important roles in these processes by transducing mechanical inputs into electrical signals [1,2]. Members of the transient receptor potential (TRP) channel superfamily have been implicated in a wide range of mechanotransduction in diverse organs and species [1]. Mammalian TRP channels are grouped into six subfamilies based on amino acid sequence homology and biophysical and pharmacological properties: TRPC (canonical or classic), TRPV (vanilloid), TRPM (melastatin), TRPML (mucolipin), TRPA (ankyrin) and TRPP (polycystin) [3]. Within the TRPV subfamily, there are six mammalian members, TRPV1–6. Among them, TRPV1 through 4 are known to be regulated by physical factors such as hypotonicity, stretch and/or temperature [4,5]. Pertinent to this study, TRPV4 is activated by shear stress generated by fluid flow and its function as a renal tubular fluid flow sensor has been demonstrated [6–9]. TRPV5 and 6 are homologous proteins with ~70% amino acid sequence homology and present in many epithelial tissues including the kidney [10]. Compared to other TRPV subfamily members, TRPV5 and 6 are highly Ca^{2+}-selective with the relative Ca^{2+} to Na^+ permeability ~100 [11]. TRPV5 and 6 channels are regulated by diverse mechanisms including Ca^{2+}, Mg^{2+}, proton, PIP_2 and protein kinases [12]. Mechanosensitivity for TRPV5 and 6 and their regulation by fluid flow and shear stress have not been described.

Normally, the kidney is the principal organ in the body for excreting dietary K^+ load. Renal K^+ excretion occurs predominantly by secretion in the distal renal tubular segments including late distal convoluted tubule (DCT2), connecting tubule (CNT), and cortical collecting duct (CCD) collectively referred to as the aldosterone-sensitive distal nephron (ASDN) [13]. The final step of K^+ secretion in ASDN involves efflux into luminal space through the apical K^+ channels, which include the renal outer medullary K^+ channel ROMK1 and the Ca^{2+}-activated maxi-K channels. ROMK is constitutively open at baseline and mainly responsible for K^+ secretion at low luminal flow rate. Maxi-K is quiescent at baseline but activated by high fluid flow and mainly responsible for flow-stimulated K^+ secretion [14].

Flow-stimulated Ca^{2+} influx across the apical membrane is requisite for flow-mediated K^+ secretion via maxi-K channel in ASDN. Several channels including TRPV4 and polycystin-2 (TRPP2) have been proposed as candidates for apical Ca^{2+} entry channels [7–9,15,16]. In addition, TRPV4 and TRPP2 may form a polymodal sensory channel complex and both or each channel subunit may be responsible for activation by flow [7,16]. TRPV5 and 6 are also expressed in apical membrane of

* Correspondence to: S.K. Cha, Department of Physiology, Yonsei University Wonju College of Medicine, 20 Ilsan-ro, Wonju, Gangwondo, South Korea. Tel.: +82 33 741 0295; fax: +82 33 745 6461.
** Correspondence to: C.L. Huang, UT Southwestern Medical Center, Department of Internal Medicine, 5323 Harry Hines Blvd., Dallas, TX 75390-8856, USA. Tel.: +1 214 648 8627; fax: +1 214 648 2071.
E-mail addresses: skcha@yonsei.ac.kr (S.-K. Cha), Chou-Long.Huang@UTSouthwestern.edu (C.-L. Huang).

0167-4889/$ – see front matter © 2013 Elsevier B.V. All rights reserved.
http://dx.doi.org/10.1016/j.bbamcr.2013.08.017

ASDN and mediate transcellular Ca^{2+} reabsorption in this part of nephron [12]. Here, we report that TRPV5 and TRPV6 are activated by fluid flow and flow-induced Ca^{2+} influx through the channels can stimulate maxi-K channel allowing K^+ efflux and causing membrane hyperpolarization. These results suggest that TRPV5 and TRPV6 may participate in the flow-stimulated K^+ secretion in ASDN.

2. Materials and methods

2.1. DNA constructs and materials

GFP-tagged wild-type and N358Q mutant TRPV5, and ROMK1 have been described previously [17–19]. Complementary DNA for TRPV6 is in a pEGFP-N3 vector. Slo1 channel was provided by Dr Chul-Seung Park [20]. Fura2/AM was obtained from Molecular Probes® (Invitrogen, Carlsbad, CA, USA). Gramicidin D and iberiotoxin were purchased from Sigma-Aldrich Co. (St. Louis, MO, USA) and Tocris Bioscience (Bristol, UK), respectively.

2.2. Cell culture, transfection and western blot

HEK293 cells were cultured as described previously [18]. Cells were transiently transfected with cDNAs as indicated in each experiment. Transfection was performed using FuGENE-HD reagent (Roche, Somerville, NJ, USA) according to the manufacturer's instructions. In each experiment, the total amount of DNA for transfection was balanced by using empty vectors. The expression of TRPV5 and TRPV6 proteins in transfected cells was detected by western blot using a rabbit polyclonal anti-GFP antibody as described previously [18].

2.3. Application of fluid flow

Pressurized flows of solutions were applied onto the single cells through a microbarrel (inner diameter ~250 μm). The tip of barrel was placed around 100 μm from the cell. Fluid flow was gravity driven (25–85 μl/min) to generate shear stresses from 0.34 to 1.15 dyn/cm^2. The shear pressure was calculated for fluid flow in cylindrical tubes according to the equation $\tau = 6\mu Q / \pi r^3$, where τ is the shear stress or pressure (dyn/cm^2), μ represents the fluid viscosity, Q is the flow rate (ml/s), and r is the internal radius of the tube [21].

2.4. Patch-clamp recordings

TRPV5 and 6 and ROMK1 currents were recorded using the whole cell-ruptured configuration of the patch clamp technique as described previously [18,19]. The patch electrodes were coated with silicone elastomer (Sylgard 184; Dow Corning, Midland, MI, USA), fire polished on a microforge, and had resistances of 2–3 MΩ when filled with the solution described below. An Ag/AgCl pellet connected via a 3 M KCl/agar bridge was used to ground the bath. The cell membrane capacitance and series resistance were compensated (>80%) electronically using an Axopatch-200B amplifier (Axon Instruments, Foster City, CA, USA). Data acquisition was performed using ClampX9.2 software (Axon Instruments). Currents were low-pass filtered at 2 kHz using 8-pole Bessel's filter in the amplifier, sampled every 0.1 ms with Digidata 1300 interface.

For measuring membrane potential, current-clamp recordings were performed under the gramicidin-perforated whole cell configuration of the patch-clamp technique using an EPC-9 amplifier and Pulse/Pulsefit (v8.50) software (HEKA Electronik, Lambrecht, Germany). A stock solution of gramicidin D was prepared at 50 mg/ml in dimethylsulfoxide and diluted in the pipette solution to a final concentration of 50 μg/ml before use. All electrophysiological recordings were performed at room temperature (~20–24 °C).

2.5. Solutions for electrophysiological recordings

For recording of TRPV5 and 6 currents, the pipette and bath solution contained (in mM) 140 Na-Asp (sodium aspartate), 10 NaCl, 10 EDTA, and 10 HEPES (pH 7.4) and 140 Na-Asp, 10 NaCl, 1 EDTA, and 10 HEPES (pH 7.4), respectively. For the recording of ROMK1 current, the pipette and bath solution contained (in mM) 140 KCl and 10 HEPES (pH 7.2) and 140 KCl, 1 $MgCl_2$, 1 $CaCl_2$, and 10 HEPES (pH 7.4), respectively.

For current-clamp recordings, patch pipettes were filled with a solution containing (in mM) 140 KCl, 5 EGTA, 10 HEPES, 0.5 $CaCl_2$, and 5 NaCl (pH 7.2). A normal physiological salt solution (PSS) was used for bath solution that contained 135 NaCl, 5.4 KCl, 1 $MgCl_2$, 2 $CaCl_2$, 5 HEPES, and 10 glucose (pH 7.4).

2.6. Intracellular Ca^{2+} ($[Ca^{2+}]_i$) measurement

Intracellular Ca^{2+} concentration ($[Ca^{2+}]_i$) was measured using Ratiomaster (Photon Technology International, Lawrencevill, NJ, USA) or the Lambda DG-4 (Sutter Instruments, Novato, CA, USA) fluorescence measurement system. Cells were placed on glass coverslips and loaded with fura-2/AM in a normal PSS in darkness for 1 h at room temperature. After dye loading, cells were washed and transferred to a perfusion chamber on a fluorescence microscope. Fura-2 signals were obtained by alternating excitation at 340 or 380 nm, and detecting emission at 510 nm. The fura-2 fluorescence ratio was calibrated to $[Ca^{2+}]_i$ as described by Grynkiewicz et al. [22]. Data were analyzed using either Felix (Photon Technology International) or MetaFluor (Sutter Instruments) software.

2.7. Data analysis

Data are presented as mean ± SEM. Statistical comparisons between two groups of data were made using a two-tailed unpaired Student's *t*-test. Multiple comparisons were determined using one-way ANOVA followed by Tukey's multiple comparison tests. Statistical significance was defined as $p < 0.05$ for a single comparison and $p < 0.01$ for multiple comparisons.

3. Results

3.1. Fluid flow activates TRPV5 and increases TRPV5-mediated Ca^{2+} influx

In previous experiments, we observed that TRPV5 currents increased consistently during fast exchanges of bath solution. This observation prompted us to carry out the present study to examine the effect of fluid flow on the activity of TRPV5 channels. In the absence of Ca^{2+}, TRPV5 conducts Na^+ [23]. We first measured TRPV5 channel activity using Na^+ as the charge carrier. TRPV5-mediated Na^+ currents (evoked by repetitive ascending ramp pulses) were measured in TRPV5 or mock-transfected human embryonic kidney (HEK)-293 cells by ruptured whole-cell patch clamp recordings. Fluid flow was applied onto the single whole cell-patched cell using a micropipette with an inner diameter of 250 μm placed ~100 μm from the cell. Without fluid flow, large inwardly rectifying currents characteristic for TRPV5 were detected in TRPV5-transfected, but not mock-transfected cells (Fig. 1A and B). Exposure of cells to fluid flow estimated to generate a physiologically relevant shear force ~1.15 dyn/cm^2 [6,9] increased TRPV5 current without altering its current–voltage (I–V) relationship. Fluid flow did not induce currents in mock transfected cells. Notably, flow-induced activation of TRPV5 was reversible and did not desensitize over 2 min (Fig. 1C and D; see also Fig. 1G). TRPV5 is a highly Ca^{2+} selective channel. The physiological function of TRPV5 is to mediate Ca^{2+} influx and thus transcellular Ca^{2+} reabsorption in the kidney. We next examined whether fluid flow increases Ca^{2+} influx via TRPV5. TRPV5-mediated Ca^{2+} influx was evident by the finding that application of 2 mM $[Ca^{2+}]$ in the bath solution increased intracellular $[Ca^{2+}]$ ($[Ca^{2+}]_i$)

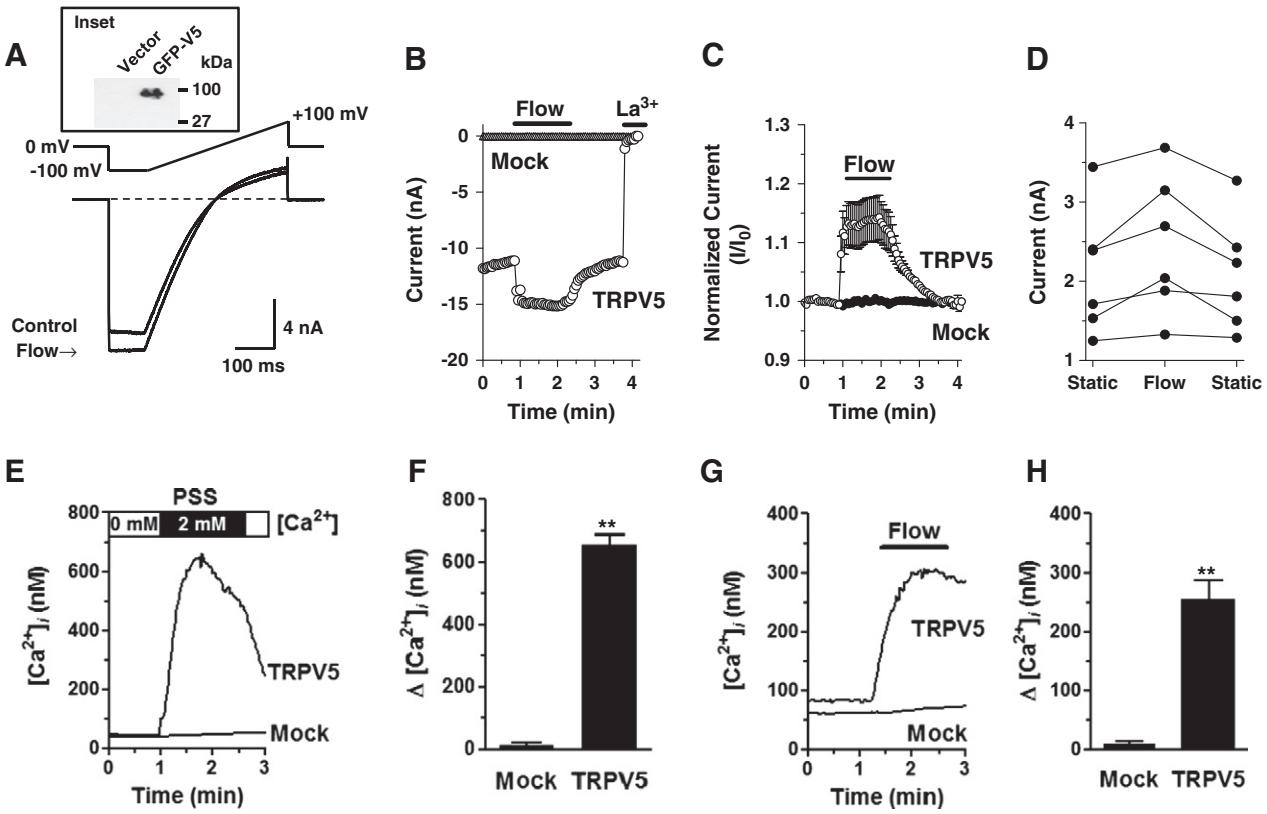

Fig. 1. Fluid flow activates TRPV5 current and Ca^{2+} influx. A, effect of fluid flow on TRPV5 current that was recorded in HEK293 cells transiently transfected with GFP-tagged TRPV5. The expression of TRPV5 protein was confirmed by immunoblot analysis by using antibody against GFP (inset). TRPV5 current was evoked by ramp pulses (applied every 2 s) from −100 to +100 mV as indicated. Ramp I–V curves of current showed typical inwardly rectifying TRPV5 current. Fluid flow pressure (~1.15 dyn/cm^2) was applied on the single cell through a micropipette. B, application of fluid flow increased current (inward current at −100 mV) in cell expressing GFP-TRPV5 (TRPV5) but not in empty vector transfected cell (Mock). Flow-stimulated current was blocked by La^{3+}, a blocker for TRPV5. C, time course of TRPV5 current in response to flow. Current amplitude (I / I_0) shown is normalized (inward current amplitude at −100 mV relative to the amplitude at starting point of recording). Data points are mean ± SEM (n = 6 each). D, individual cell response to flow. Inward current (at −100 mV) at no fluid flow (static), application of fluid flow and back to static. E, representative traces illustrating time course of $[Ca^{2+}]_i$ response to application of 2 mM Ca^{2+} in the bath. Cells were incubated with a Ca^{2+}-free physiological salt solution (PSS, see Materials and methods for composition) before application of 2 mM Ca^{2+} in bath. F, summary of 2 mM Ca^{2+}-induced change in $[Ca^{2+}]_i$, $\Delta[Ca^{2+}]_i$. G, representative traces showing flow-induced $[Ca^{2+}]_i$ responses which were measured with normal PSS in TRPV5- or mock-transfected cell. H, summary of results in panel G. $\Delta[Ca^{2+}]_i$ denotes change of $[Ca^{2+}]_i$. Data points (F and H) are the mean ± SEM (n = 20). Double asterisk denotes $p < 0.01$ versus Mock.

measured by fura-2 fluorescence in HEK293 cell expressing TRPV5 but not in mock transfected cells (Fig. 1E and F). Fluid flow increased $[Ca^{2+}]_i$ in cells expressing TRPV5 but not in mock cell (Fig. 1G and H), supporting the notion that flow stimulates TRPV5-mediated Ca^{2+} influx.

We next examined the dynamic range of shear force for activation of TRPV5. Incremental increases in fluid flow rate that generates shear force from 0.34 to 1.15 dyn/cm^2 caused an immediate and step-wise increase of TRPV5 current (Fig. 2A and B). These results indicate that the activity of TRPV5 channels can dynamically vary in response to physiological alterations of luminal flow rate in vivo. In subsequent experiments throughout the paper, we used flow rate with shear force ~1.15 dyn/cm^2.

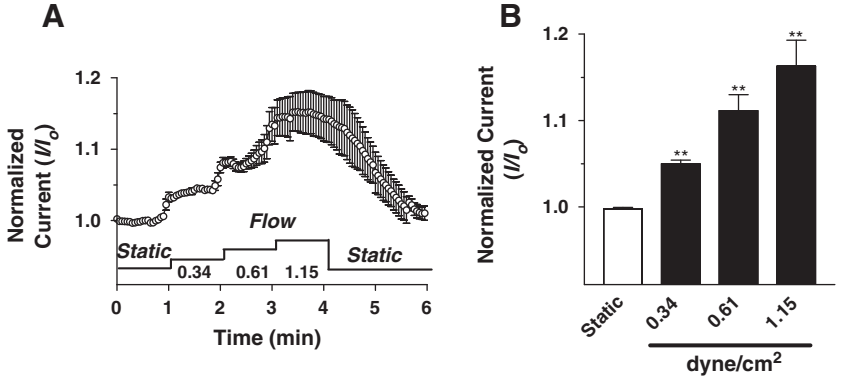

Fig. 2. Flow-dependent graded activation of TRPV5. A, changes of TRPV5 current under different rates of fluid flow. Shown is normalized current amplitude (I / I_0). Flow rates that generate shear force equivalent to 0.34, 0.61 and 1.15 dyn/cm^2 were studied. B, summary of results in panel A (mean ± SEM, n = 6). Data points are mean ± SEM (n = 6). Double asterisk denotes $p < 0.01$ versus static state.

3.2. Glycosylation of TRPV5 is important for flow-induced activation of TRPV5

The asparagines-358 of TRPV5 is in the extracellular domain and the only site for N-linked glycosylation [17,24]. N-glycans of channels may interact with the extracellular matrix and proteins and thereby participate in mechanosensation [5,25,26]. To explore the possibility that N-glycan of TRPV5 may be involved in the flow stimulation of channel activity, we studied the effect of fluid flow on wild-type and N-glycosylation defective mutant that carries Asn-358 to glutamine (N358Q) mutation. TRPV5-mediated currents and $[Ca^{2+}]_i$ levels increased in cells expressing wild-type channels in response to fluid flow (Fig. 3). In contrast, fluid flow-stimulated increases of currents and Ca^{2+} influx were blunted in cells expressing N358Q-TRPV5 mutant channel. The basal TRPV5 currents (Na^+ as the charge carrier, in the absence of fluid flow) were not different between cells expressing wild-type and N358Q mutant (9.05 ± 0.92 nA vs 9.17 ± 0.94 nA, WT vs N358Q). Previously, we have also shown that current density and cell surface expression of the N358Q mutant were not different from those of wild-type TRPV5 [17]. Thus, the extracellular N-glycan of TRPV5 is important for flow stimulation of the channel.

3.3. Flow-dependent activation of TRPV5 induces Slo1-mediated hyperpolarization

Maxi-K channels are normally relatively quiescent at the resting membrane potential and the resting intracellular Ca^{2+} levels, but activated by an increase of $[Ca^{2+}]_i$ and/or membrane depolarization. Maxi-K channels are responsible for flow-stimulated K^+ secretion in the distal nephron. We next examined functional coupling between TRPV5-mediated Ca^{2+} entry and activation of maxi-K. HEK cells were transfected with TRPV5 and/or the pore-forming α-subunit of *Slo1*-encoded maxi-K, and membrane potentials were recorded in perforated whole-cell mode under current clamp (Fig. 4A). HEK293 is a non-excitable cell line. The resting membrane potential of these cells recorded in the basal state with normal physiological salt solution was around −15 to −20 mV (Fig. 4B). Fluid flow caused membrane depolarization in TRPV5-transfected cells, presumably from increased Ca^{2+} influx through the channel (Fig. 4A–C). In contrast, cells coexpressing TRPV5 and Slo1 α subunit developed membrane hyperpolarization in response to fluid flow, supporting that flow-stimulated Ca^{2+} influx stimulates K^+ efflux through *Slo1*-encoded maxi-K channels causing membrane hyperpolarization. In support of this notion, fluid flow had no effect on membrane potentials in cells transfected by Slo1 α subunit alone (Fig. 4A–C) or in mock-transfected cells (not shown). Furthermore, preincubation of cells coexpressing TRPV5 and Slo1 α subunit with a maxi-K-specific blocker iberiotoxin (IBTX) prevented flow-induced membrane hyperpolarization (via maxi-K), leaving only membrane depolarization through TRPV5 (Fig. 4D–F). Also, preventing Ca^{2+} influx through TRPV5 by application of a blocker La^{3+} markedly inhibited membrane hyperpolarization (Fig. 4D–F).

3.4. Flow activates TRPV6 current and Ca^{2+} influx causing Slo1-mediated hyperpolarization

TRPV6 is another highly Ca^{2+} selective channel closely related to TRPV5. TRPV6 partially colocalizes with TRPV5 in the apical membrane of distal nephron and may form heteromultimers with TRPV5 [27]. We examined whether TRPV6 is also sensitive to flow and Ca^{2+} influx through TRPV6 can activate Slo1 maxi-K channel. As was for TRPV5, increases in fluid flow stimulated Na^+ currents (Fig. 5A and B) and Ca^{2+} influx (Fig. 5C–E) in HEK293 cells expressing TRPV6 but not in mock transfected cells. Flow-induced increases of TRPV6 current and Ca^{2+}

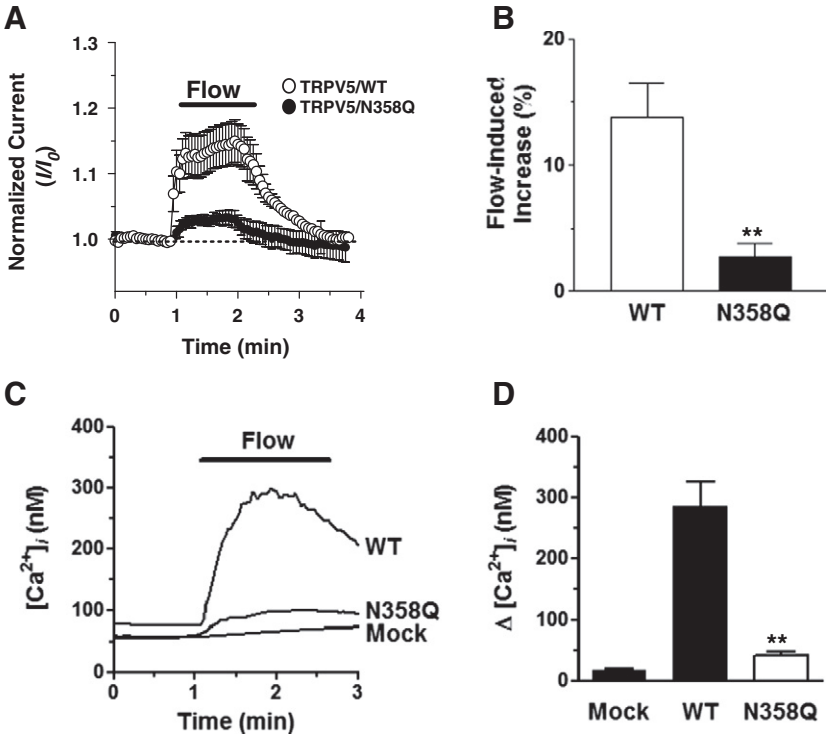

Fig. 3. Role of N-glycosylation of TRPV5 in flow-mediated activation of the channel. A, time course of current activation by fluid flow for wild-type (WT) and N358Q mutant. B, summary of results in panel A (mean ± SEM, $n = 6$). Double asterisk denotes $p < 0.01$ versus WT. C, representative traces illustrating flow-induced $[Ca^{2+}]_i$ responses recorded in cells expressing WT or N358Q TRPV5 or mock-transfected cells. $[Ca^{2+}]_i$ was measured using fura-2 fluorimetry in the normal PSS. D, summary of results in panel C (mean ± SEM, $n = 6$). Double asterisk denotes $p < 0.01$ versus WT or Mock. To exclude that GFP tag affects flow-induced response of TRPV5, we found that the flow-induced $[Ca^{2+}]_i$ changes ($\Delta[Ca^{2+}]_i$) were not different between cells expressing GFP-tagged and non-tagged TRPV5 (314 ± 33 nM vs 323 ± 35 nM) (data not illustrated in graph here).

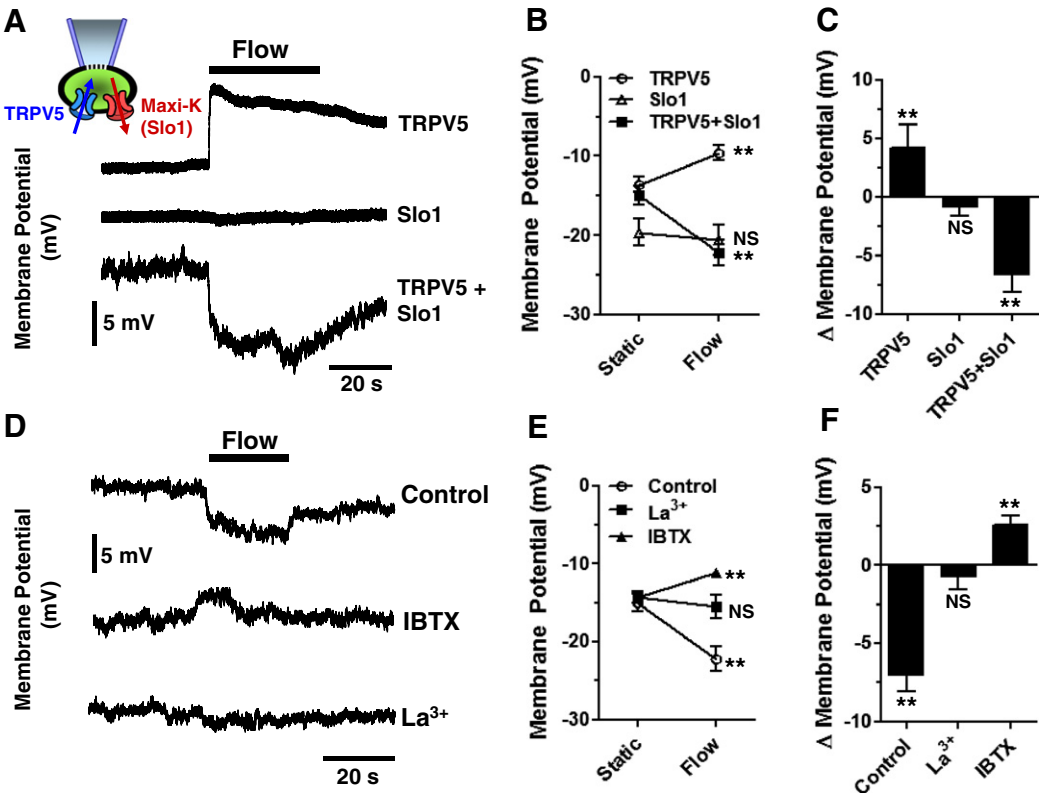

Fig. 4. Flow-mediated activation of TRPV5 induces Slo1-mediated membrane hyperpolarization. Membrane potential was measured using current-clamp recording under gramicidin-perforated whole-cell configuration of patch-clamp technique in normal PSS. A, representative traces showing effects of flow on membrane potential changes in cells expressing individual TRPV5 or Slo1 or both. B, resting membrane potentials during static and during flow as in panel A (mean ± SEM, $n = 6$). Double asterisk denotes $p < 0.01$, static versus flow. NS, statistically not significant. C, summary of membrane potential changes in panel A (mean ± SEM, $n = 6$). Positive and negative flow-induced membrane potential changes (ΔMembrane Potential [mV]) reflect membrane depolarization and hyperpolarization, respectively. Double asterisk denotes $p < 0.01$ versus 0 mV membrane potential changes. NS, statistically not significant. D, representative traces showing effect of Slo1 and TRPV5 blocker, iberiotoxin (IBTX, 200 nM) and La^{3+} (100 μM), respectively, on flow-induced membrane potential changes in cells expressing both TRPV5 and Slo1. E, resting membrane potentials during static and during flow as in panel D (mean ± SEM, $n = 7–12$). Double asterisk denotes $p < 0.01$, static versus flow. NS, statistically not significant. F, summary of membrane potential changes in panel D (mean ± SEM, $n = 7–12$). Positive and negative flow-induced membrane potential changes (ΔMembrane Potential [mV]) reflect membrane depolarization or hyperpolarization, respectively. Double asterisk denotes $p < 0.01$ versus no (0 mV) membrane potential changes. NS, statistically not significant.

influx were reversible as was for TRPV5. Results of experiments using IBTX and La^{3+} support the notion that TRPV6-mediated Ca^{2+} influx also activated K^+ efflux through *Slo1*-encoded maxi-K channel (Fig. 5F–H). Thus, flow-stimulated increases in $[Ca^{2+}]_i$ mediated by both TRPV6 and TRPV5 can activate maxi-K.

3.5. ROMK channel is insensitive to shear stress

ROMK K^+ channel is constitutively open at the resting membrane potential and intracellular Ca^{2+} level and believed to mediate the basal, non-flow stimulated K^+ secretion in the distal nephron. We examined the effect of flow on ROMK1 channel activity. Ruptured whole-cell recording revealed that HEK293 cells transfected with ROMK1 exhibited characteristic inwardly rectifying K^+ currents (Fig. 6A). Fluid flow had no effect on current amplitude of ROMK1 and its I–V relationship (Fig. 6A–C). Mock transfected cells did not display inwardly rectifying K^+ current and had no response to fluid flow (Fig. 6B and C). The resting membrane potential of HEK cells expressing ROMK (recorded in perforated whole-cell mode under current clamp) was more negative than those of mock-transfected cells in the basal state (-68.5 ± 1.9 mV vs -20.8 ± 1.6 mV, $p < 0.01$; $n = 12$ each), indicating that ROMK channel is constitutively open thus clamping the resting membrane potential toward equilibrium potential for K^+. Indeed, blocking ROMK by Ba^{2+} in ROMK-transfected cell restored membrane potentials to the level of untransfected cells (Fig. 6D). Fluid flow in cells coexpressing TRPV5 and ROMK caused membrane depolarization (Fig. 6E and F) as observed in cells expressing TRPV5 alone (Fig. 4A), rather than hyperpolarization as observed in cells coexpressing TRPV5 and Slo1. Thus, ROMK is not activated by increases in $[Ca^{2+}]_i$ nor stimulated by fluid flow.

4. Discussion

It is well established that Ca^{2+}-activated K^+ channels play an important role in flow-stimulated K^+ secretion in distal nephron. Both Ca^{2+} entry through apical Ca^{2+}-permeable channels and intracellular Ca^{2+} release have been shown to be important for stimulating Ca^{2+}-activated K^+ channel for flow-stimulated renal K^+ secretion [28]. With respect to apical Ca^{2+} entry, several TRP channels have been proposed for this role. These include TRPV4, TRPV4–TRPP2 complex, and heteromeric TRPP1–TRPP2 channels [6–9,15]. TRPV5 is expressed in DCT2 and CNT whereas TRPV6 is located from DCT2 to CCD and both channels are believed to be responsible for transcellular Ca^{2+} reabsorption in the distal nephron. In the present study, we show that TRPV5 and TRPV6 channels are activated by shear force generated by fluid flow. The activity of the channels varies dynamically with changes of fluid flow rate within the range observed in physiological settings (shear force between 0.34 and 1.15 dyn/cm^2, see below). We further show that flow-stimulated Ca^{2+} influx through TRPV5 and TRPV6 is sufficient to activate *Slo1*-encoded Ca^{2+}-activated maxi-K, which are present in DCT2 and CNT where flow-stimulated K^+ secretion is known to take place [29]. Thus, our results suggest that TRPV5 and

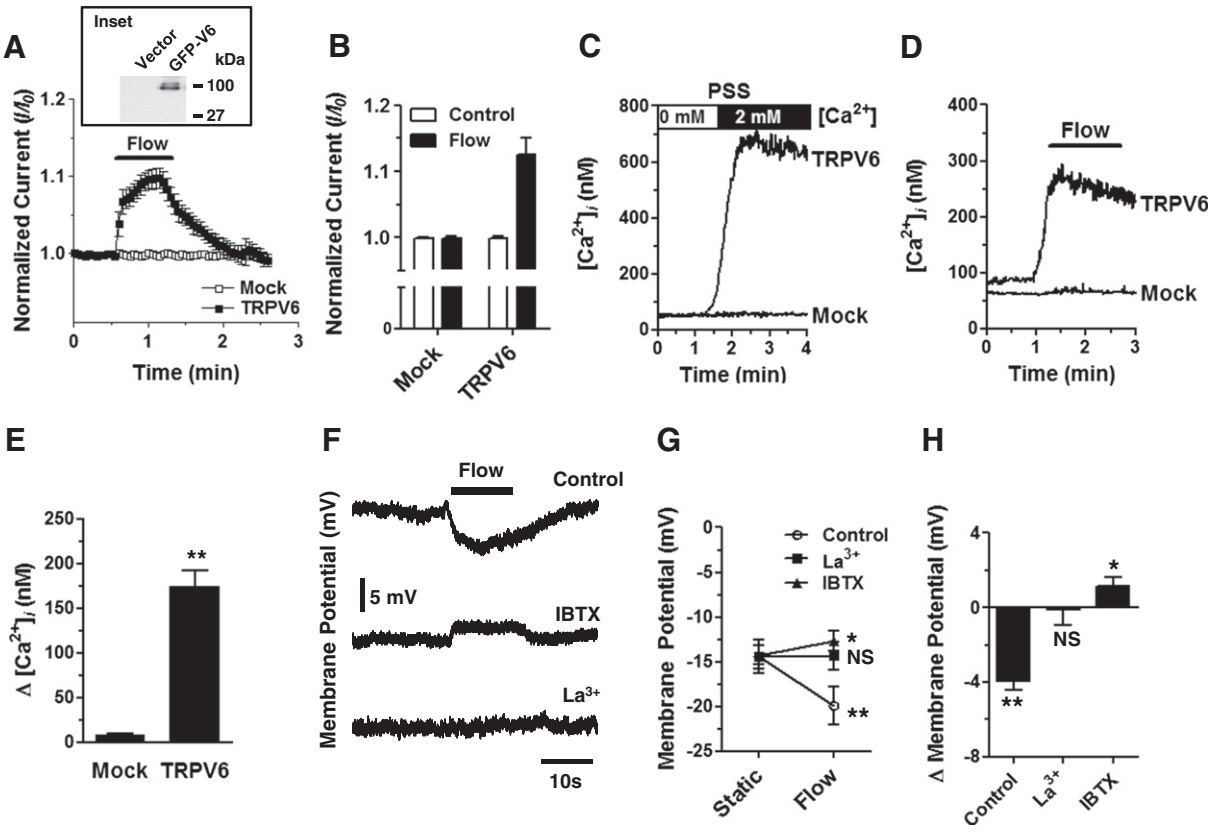

Fig. 5. Flow activates TRPV6 causing Slo1-mediated membrane hyperpolarization. A, effect of fluid flow on TRPV6 current that was recorded in HEK293 cells transiently transfected with GFP-tagged TRPV6. The expression of TRPV6 protein in transfected cells was confirmed by western blot analysis (inset). TRPV6 current was evoked by ramp pulses from −100 to +100 mV as was for TRPV5. B, summarized results as in panel A (mean ± SEM, $n = 6$ each). C, representative traces for $[Ca^{2+}]_i$ responses by bath application of 2 mM Ca^{2+} in cells expressing GFP-TRPV6 or empty vector (Mock). Cells were incubated Ca^{2+}-free PSS before bath perfusion of 2 mM Ca^{2+}. D, representative traces for flow-induced $[Ca^{2+}]_i$ responses in TRPV6 or mock cells in the presence of 2 mM Ca^{2+} in bath. E, summary of flow-induced change in $[Ca^{2+}]_i$, $\Delta[Ca^{2+}]_i$ in panel 5D (mean ± SEM, $n = 30$). Double asterisk denotes $p < 0.01$ versus Mock. F, representative traces of membrane potential of cells coexpressing TRPV6 and Slo1 in response to fluid flow in the presence or absence of IBTX (200 nM) or La^{3+} (100 μM). G, resting membrane potential during static and during flow in panel F (mean ± SEM, $n = 6$). Asterisk and double asterisk denote $p < 0.05$ and $p < 0.01$, respectively, static versus flow. NS, statistically not significant. H, summary of changes of membrane potentials in panel F (mean ± SEM, $n = 6$). Positive and negative flow-induced membrane potential changes (ΔMembrane Potential [mV]) reflect membrane depolarization and hyperpolarization, respectively. Asterisk and double asterisk denote $p < 0.05$ and $p < 0.01$, respectively, versus no (0 mV) membrane potential changes. NS, statistically not significant.

TRPV6-mediated Ca^{2+} entry may contribute to the mechanism of flow-stimulated K^+ secretion in DCT2 and CNT.

Several studies have reported on physiologically relevant shear force generated by fluid flow and shear force required for the activation of mechanosensitive channels in renal tubules. It is estimated that shear force generated by fluid flow in CCD ranges from 0.5 to >20 dyn/cm^2 with typical values between 1 and 10 dyn/cm^2 [6,9,30]. TRPV4 channels can be activated by 1–3 dyn/cm^2 of laminar shear stress [6]. Heteromeric TRPV4–TRPP2 channels can be activated by 0.5 dyn/cm^2 [7]. Our results that TRPV5 is activated by shear force between 0.34 and 1.15 dyn/cm^2 support the notion that flow activation of TRPV5 is physiologically relevant. The role of TRPV4 in flow-induced $[Ca^{2+}]_i$ increase was examined in CCD [6,8]. Whether TRPV4 is expressed in DCT2 and CNT and its role in flow-stimulated K^+ secretion in these segments with or without heteromerization with TRPV5 or TRPV6 are unknown.

Activation of TRPV5 or TRPV6 by fluid flow can also contribute to K^+ secretion independently of intracellular Ca^{2+}-mediated stimulation of maxi-K channels. K^+ efflux across the apical membrane causes membrane hyperpolarization, limiting maximal K^+ secretion. Increases in distal Na^+ delivery and activation of the epithelial Na^+ channel ENaC by enhanced flow [31] cause apical depolarization and provide the driving force for K^+ secretion. Membrane depolarization resulting from flow stimulation of TRPV5 and TRPV6 as we observed in this study may provide further augmentation of driving force for K^+ secretion.

Our findings may also have implications to the mechanism of thiazide-induced hypocalciuria. Volume contraction with increased proximal Ca^{2+} reabsorption plays an important role in hypocalciuria during chronic thiazide treatment [32]. However, increased proximal Ca^{2+} reabsorption from volume contraction is unlikely the only mechanism for hypocalciuria because it can develop acutely after a single dose of hydrochlorothiazide [33]. It is conceivable that increases in fluid flow in DCT2 and CNT that resulted from inhibition of Na–Cl cotransporter by thiazide may stimulate Ca^{2+} reabsorption through TRPV5 and 6 causing hypocalciuria.

In this study, we have also begun to explore the molecular mechanism of flow-induced activation of TRPV5. Recent studies reported that N-glycosylation defective TRPV4 exhibited decreased flow- and/or hypotonicity-induced Ca^{2+} influx [34,35]. We have previously reported that the disaccharide N-acetyllactosamine in the N-glycan chain of TRPV5 is a ligand for galectin-1 residing on the extracellular surface of cell membrane [17]. Interaction of TRPV5 with galectin-1 via the N-glycan plays an important role in the retention of channels on the cell surface. Here, we show that N-glycan-deficient TRPV5 mutant is much less sensitive to stimulation by fluid flow. Future studies will investigate the hypothesis that the interaction between N-glycan of TRPV5 and galectin-1 is important for mechanosensitivity of the channel, perhaps by providing anchoring and specific structural orientation to the channel that may be amiable to perturbation by fluid flow.

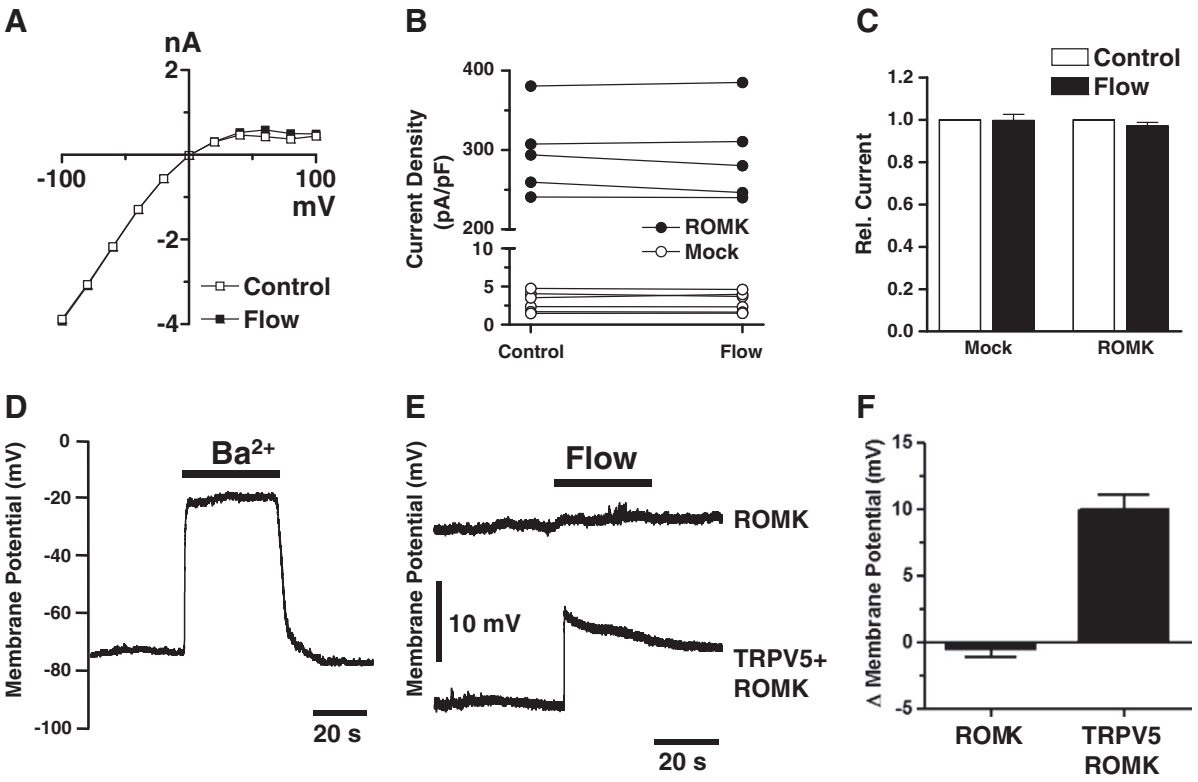

Fig. 6. Effect of flow on ROMK1. A, I–V curves of currents in cells expressing ROMK1 under control (no flow) or fluid flow. B, current densities at −100 mV (normalized to the cell surface area; pA / pF) in ROMK1- or mock-transfected cells under control or fluid flow. C, summary of results in panel B (mean ± SEM, $n = 5$–6). D, representative traces of membrane potential of cell expressing ROMK in response to application of Ba^{2+} (1 mM). E, representative traces showing effects of fluid flow on membrane potential changes in cells expressing ROMK alone or both ROMK and TRPV5. F, summary of results in panel E (mean ± SEM, $n = 8$–10).

Acknowledgements

This study was supported by the Basic Science Research Program through the National Research Foundation of Korea funded by the Ministry of Education, Science and Technology (Grant 2010-0024789 to S.-K. C.), a research grant from the Yonsei University Wonju College of Medicine (Grant YUWCM-2010-7-0482 to S.-K.C.), and the National Institutes of Health of USA (DK-85726 to C.-L.H). C.-L.H holds the Jacob Lemann Professorship in Calcium Transport of University of Texas Southwestern Medical Center. We thank Dr Chul-Seung Park for Slo1 plasmid.

References

[1] A.P. Christensen, D.P. Corey, TRP channels in mechanosensation: direct or indirect activation? Nat. Rev. Neurosci. 8 (2007) 510–521.
[2] A. Patel, R. Sharif-Naeini, J.R. Folgering, D. Bichet, F. Duprat, E. Honoré, Canonical TRP channels and mechanotransduction: from physiology to disease states, Pflugers Arch. 460 (2010) 571–581.
[3] L.J. Wu, T.B. Sweet, D.E. Clapham, International Union of Basic and Clinical Pharmacology. LXXVI. Current progress in the mammalian TRP ion channel family, Pharmacol. Rev. 62 (2010) 381–404.
[4] J. Yin, W.M. Kuebler, Mechanotransduction by TRP channels: general concepts and specific role in the vasculature, Cell Biochem. Biophys. 56 (2010) 1–18.
[5] A.J. Kuipers, J. Middelbeek, F.N. van Leeuwen, Mechanoregulation of cytoskeletal dynamics by TRP channels, Eur. J. Cell Biol. 91 (2012) 834–846.
[6] J. Berrout, M. Jin, M. Mamenko, O. Zaika, O. Pochynyuk, R.G. O'Neil, Function of transient receptor potential cation channel subfamily V member 4 (TRPV4) as a mechanical transducer in flow-sensitive segments of renal collecting duct system, J. Biol. Chem. 287 (2012) 8782–8791.
[7] J. Du, W.J. Wong, L. Sun, Y. Huang, X. Yao, Protein kinase G inhibits flow-induced Ca^{2+} entry into collecting duct cells, J. Am. Soc. Nephrol. 23 (2012) 1172–1180.
[8] J. Taniguchi, S. Tsuruoka, A. Mizuno, J. Sato, A. Fujimura, M. Suzuki, TRPV4 as a flow sensor in flow-dependent K^+ secretion from the cortical collecting duct, Am. J. Physiol. Renal Physiol. 292 (2007) F667–F673.
[9] L. Wu, X. Gao, R.C. Brown, S. Heller, R.G. O'Neil, Dual role of the TRPV4 channel as a sensor of flow and osmolality in renal epithelial cells, Am. J. Physiol. Renal Physiol. 293 (2007) F1699–F1713.
[10] D.E. Clapham, TRP channels as cellular sensors, Nature 426 (2003) 517–524.
[11] R. Vennekens, J.G. Hoenderop, J. Prenen, M. Stuiver, P.H. Willems, G. Droogmans, B. Nilius, R.J. Bindels, Permeation and gating properties of the novel epithelial Ca^{2+} channel, J. Biol. Chem. 275 (2000) 3963–3969.
[12] J.G. Hoenderop, R.J. Bindels, Calciotropic and magnesiotropic TRP channels, Physiology (Bethesda) 23 (2008) 32–40.
[13] T. Rieg, V. Vallon, M. Sausbier, U. Sausbier, B. Kaissling, P. Ruth, H. Osswald, The role of the BK channel in potassium homeostasis and flow-induced renal potassium excretion, Kidney Int. 72 (2007) 566–573.
[14] A.R. Rodan, C.L. Huang, Distal potassium handling based on flow modulation of maxi-K channel activity, Curr. Opin. Nephrol. Hypertens. 18 (2009) 350–355.
[15] S.M. Nauli, F.J. Alenghat, Y. Luo, E. Williams, P. Vassilev, X. Li, A.E. Elia, W. Lu, E.M. Brown, S.J. Quinn, D.E. Ingber, J. Zhou, Polycystins 1 and 2 mediate mechanosensation in the primary cilium of kidney cells, Nat. Genet. 33 (2003) 129–137.
[16] M. Köttgen, B. Buchholz, M.A. Garcia-Gonzalez, F. Kotsis, X. Fu, M. Doerken, C. Boehlke, D. Steffl, R. Tauber, T. Wegierski, R. Nitschke, M. Suzuki, A. Kramer-Zucker, G.G. Germino, T. Watnick, J. Prenen, B. Nilius, E.W. Kuehn, G. Walz, TRPP2 and TRPV4 form a polymodal sensory channel complex, J. Cell Biol. 182 (2008) 437–447.
[17] S.K. Cha, B. Ortega, H. Kurosu, K.P. Rosenblatt, M. Kuro-O, C.L. Huang, Removal of sialic acid involving Klotho causes cell-surface retention of TRPV5 channel via binding to galectin-1, Proc. Natl. Acad. Sci. U. S. A. 105 (2008) 9805–9810.
[18] S.K. Cha, T. Wu, C.L. Huang, Protein kinase C inhibits caveolae-mediated endocytosis of TRPV5, Am. J. Physiol. Renal Physiol. 294 (2008) F1212–F1221.
[19] G. He, H.R. Wang, S.K. Huang, C.L. Huang, Intersectin links WNK kinases to endocytosis of ROMK1, J. Clin. Invest. 117 (2007) 1078–1087.
[20] S. Jo, K.H. Lee, S. Song, Y.K. Jung, C.S. Park, Identification and functional characterization of cereblon as a binding protein for large-conductance calcium-activated potassium channel in rat brain, J. Neurochem. 94 (2005) 1212–1224.
[21] S. Lee, J.C. Kim, Y. Li, M.J. Son, S.H. Woo, Fluid pressure modulates L-type Ca^{2+} channel via enhancement of Ca^{2+}-induced Ca^{2+} release in rat ventricular myocytes, Am. J. Physiol. Cell Physiol. 294 (2008) C966–C976.
[22] G. Grynkiewicz, M. Poenie, R.Y. Chen, A new generation of Ca^{2+} indicators with greatly improved fluorescence properties, J. Biol. Chem. 260 (1985) 3440–3450.
[23] B. Nilius, R. Vennekens, J. Prenen, J.G. Hoenderop, R.J. Bindels, G. Droogmans, Whole-cell and single channel monovalent cation currents through the novel rabbit epithelial Ca^{2+} channel ECaC, J. Physiol. 527 (Pt 2) (2000) 239–248.
[24] Q. Chang, S. Hoefs, A.W. van der Kemp, C.N. Topala, R.J. Bindels, J.G. Hoenderop, The β-glucuronidase Klotho hydrolyzes and activates the TRPV5 channel, Science 310 (2005) 490–493.
[25] J. Ando, K. Yamamoto, Flow detection and calcium signalling in vascular endothelial cells, Cardiovasc. Res. (2013), http://dx.doi.org/10.1093/cvr/cvt084.

[26] M.E. Janik, A. Lityńska, P. Vereecken, Cell migration—the role of integrin glycosylation, Biochim. Biophys. Acta 1800 (2010) 545–555.
[27] J.G. Hoenderop, T. Voets, S. Hoefs, F. Weidema, J. Prenen, B. Nilius, R.J. Bindels, Homo- and heterotetrameric architecture of the epithelial Ca^{2+} channels TRPV5 and TRPV6, EMBO J. 22 (2003) 776–785.
[28] W. Liu, T. Morimoto, C. Woda, T.R. Kleyman, L.M. Satlin, Ca^{2+} dependence of flow-stimulated K secretion in the mammalian cortical collecting duct, Am. J. Physiol. Renal Physiol. 293 (2007) F227–F235.
[29] M.A. Bailey, A. Cantone, Q. Yan, G.G. MacGregor, Q. Leng, J.B. Amorim, T. Wang, S.C. Hebert, G. Giebisch, G. Malnic, Maxi-K channels contribute to urinary potassium excretion in the ROMK-deficient mouse model of Type II Bartter's syndrome and in adaptation to a high-K diet, Kidney Int. 70 (2006) 51–59.
[30] Z. Cai, J. Xin, D.M. Pollock, J.S. Pollock, Shear stress-mediated NO production in inner medullary collecting duct cells, Am. J. Physiol. Renal Physiol. 279 (2000) F270–F274.
[31] L.M. Satlin, S. Sheng, C.B. Woda, T.R. Kleyman, Epithelial Na^{+} channels are regulated by flow, Am. J. Physiol. Renal Physiol. 280 (2001) F1010–F1018.
[32] R.F. Reilly, C.L. Huang, The mechanism of hypocalciuria with NaCl cotransporter inhibition, Nat. Rev. Nephrol. 7 (2011) 669–674.
[33] K. Stefíková, V. Spustová, R. Dzúrik, Acute effect of hydrochlorothiazide on renal calcium and magnesium handling in postmenopausal women, Physiol. Res. 48 (1999) 327–330.
[34] S.R. Lamandé, Y. Yuan, I.L. Gresshoff, L. Rowley, D. Belluoccio, K. Kaluarachchi, C.B. Little, E. Botzenhart, K. Zerres, D.J. Amor, W.G. Cole, R. Savarirayan, P. McIntyre, J.F. Bateman, Mutations in TRPV4 cause an inherited arthropathy of hands and feet, Nat. Genet. 43 (2011) 1142–1146.
[35] O. Zaika, M. Mamenko, J. Berrout, N. Boukelmoune, R.G. O'Neil, O. Pochynyuk, TRPV4 dysfunction promotes renal cystogenesis in autosomal recessive polycystic kidney disease, J. Am. Soc. Nephrol. 24 (2013) 604–616.